

Combined Raman and Photoluminescence (PL) Imaging of Two-Dimensional WS₂

David Tuschel

Combined Raman and photoluminescence (PL) spectroscopy and imaging are used to examine the spatial variation of solid-state structure and electronic character of two-dimensional (2-D) tungsten disulfide (WS₂) crystals. Simultaneous mapping acquisition of PL and Raman scattering from the same spatial locations provide complementary structural information and a way of rendering combinative Raman and PL spectral images of thin film 2-D crystals in general and WS₂ in particular.

Graphene is probably the most well-known of the emerging class of materials known as two-dimensional (2-D) crystals. These materials are constituted by monolayer to few-layered structures. In recent years, new inorganic 2-D materials have emerged, including MoS₂, MoSe₂, WS₂, and WSe₂, among others. These materials have attracted significant interest because of their special electronic, optical, and optoelectronic properties in the monolayer to few-layer forms that are different from those of the bulk form (1,2). One of the most significant differences of the 2-D crystals is the transformation from an indirect band gap semiconductor in the bulk to a direct band gap semiconductor in the monolayer to few-layer crystals. Thus, the fabrication of optoelectronic devices in addition to familiar integrated electronic circuitry is envisioned for these materials. These optoelectronic characteristics have prompted substantial research to discover the means of fabrication and the physical characteristics of 2-D crystals to produce integrated electronic and optoelectronic devices (3).

Raman and Photoluminescence (PL) Imaging of 2-D WS₂

You may have observed the spatially varying colors in reflected white light images of 2-D crystals, and so there have been

developments to use optical microscopy to rapidly identify the number of molecular layers that make up the 2-D crystal (4). Previously, we reported on the use of Raman and PL spectroscopy and imaging of few-layer MoS₂ to identify spatial variation in the number of layers and strain (5–7). In this installment of “Molecular Spectroscopy Workbench,” we focus on combined Raman and PL imaging for the characterization of 2-D WS₂ crystals.

Here, we apply Raman and PL spectral imaging to reveal the spatially varying structural differences that are not observed when viewing the crystals with reflected white light microscopy. A collection of hyperspectral data acquired by spectral mapping of a 2-D WS₂ crystal is shown in Figure 1. A reflected white light image of the crystal appears in the lower right-hand corner, and a combinative Raman and photoluminescence image corresponding to the reflected light image appears to its left. The plot on the upper left consists of all the spectra acquired over the image area, and the upper right-hand plot shows the single spectrum associated with the cross-hair location in the spectral and reflected light images. Note that each spectrum covers a spectral range that includes contributions from both Raman scattering and PL. The Raman and PL data were acquired using 532 nm excitation in conjunction with a

300 gr/mm grating and a 50x Olympus objective and by moving the stage in 1.5 μm increments over an area of approximately $100\ \mu\text{m} \times 100\ \mu\text{m}$. The combinative spectral image is rendered through a color-coded plot of the spatial variation of Raman (green) and PL (red) signal strength within the corresponding color bracketed Raman shift positions shown in the two upper traces. The combinative Raman and PL image is actually a rendering of normalized (minimum to maximum) signal strength for the Raman band at $349\ \text{cm}^{-1}$ and the PL band centered primarily at $630\ \text{nm}$ as a function of position on the sample. The hyperspectral data clearly reveal the nonuniformity of the PL corresponding to a spatial variation of the intensity and peak position. Consequently, PL images could be rendered of the spatially varying peak position along with that of spatially varying signal strength.

The triangular crystal consists primarily of a single layer of WS_2 with a three-pronged two-layer formation growing out from the center. The light blue triangle in the center of the reflected white light image consists of multiple layers of WS_2 . The three-pronged two-layer formation appears darker purple in the reflected white light image and brighter green in the combinative Raman and PL spectral image, because of the greater Raman scattering and attenuated PL from the two-layer structure. The combinative spectral image is rendered through a color-coded plot of Raman (green) and PL (red) signal strength where each component's color intensity scale is normalized minimum to maximum to reveal the spatially varying contrast of both spectral components.

The separate Raman and PL images in Figure 2 show the spatially varying differences in solid state structure as revealed through vibrational and electronic spectroscopy, respectively. The three-pronged two-layer formation appears brighter in the Raman image than the rest of the single-

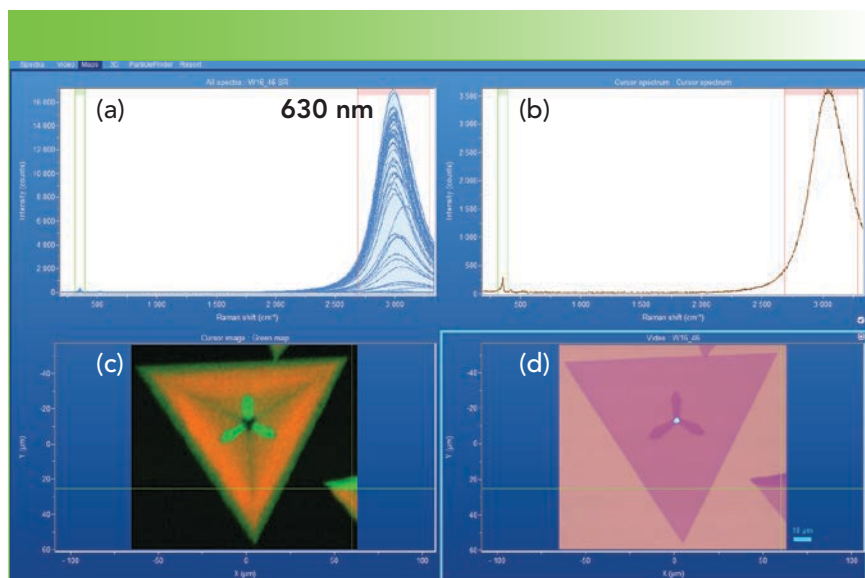


FIGURE 1: (a) hyperspectral data set, (b) cursor spectrum, (c) combinative Raman and photoluminescence image, and (d) reflected white light image of 2-D WS_2 crystal.

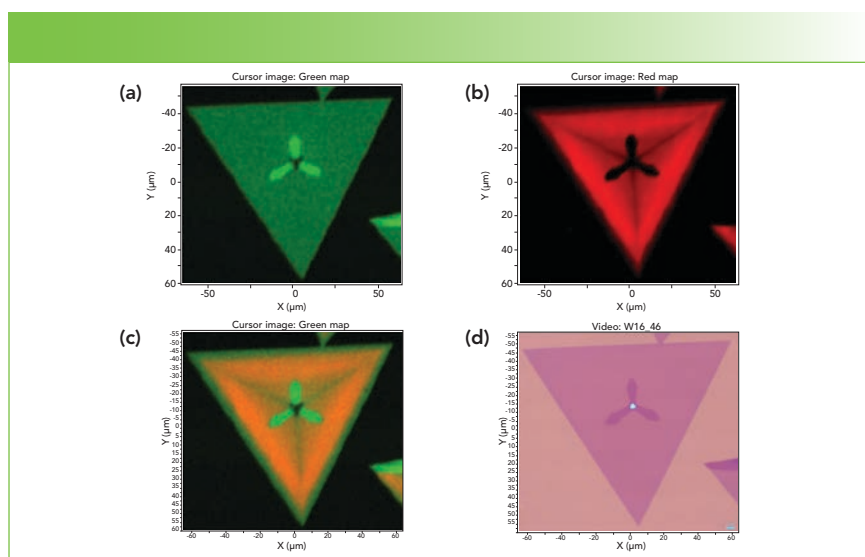


FIGURE 2: Spectral and reflected white light imaging of WS_2 : (a) Raman, (b) photoluminescence, (c) combinative Raman and photoluminescence, and (d) reflected white light image.

layer crystal, which appears uniform and dark green. The triangular feature in the center appears dark, consistent with all past reporting that many layer structures have been shown to generate much weaker Raman scattering than either single or few-layer 2-D crystals.

In contrast with the Raman image, the three-pronged two-layer formation appears dark in the PL image because of very weak emission. The diminished PL in

the surrounding single-layer area grows progressively brighter towards the crystal perimeter. Furthermore, dark lines indicating attenuated PL in the single-layer area bisect the three prongs of the two-layer formation. One can envision a triangle formed by lines perpendicular to the tips of the three two-layer prongs. A spatial variation of attenuated PL appears within that triangle. Outside of that triangle boundary, the PL is uniformly strong. Nevertheless,

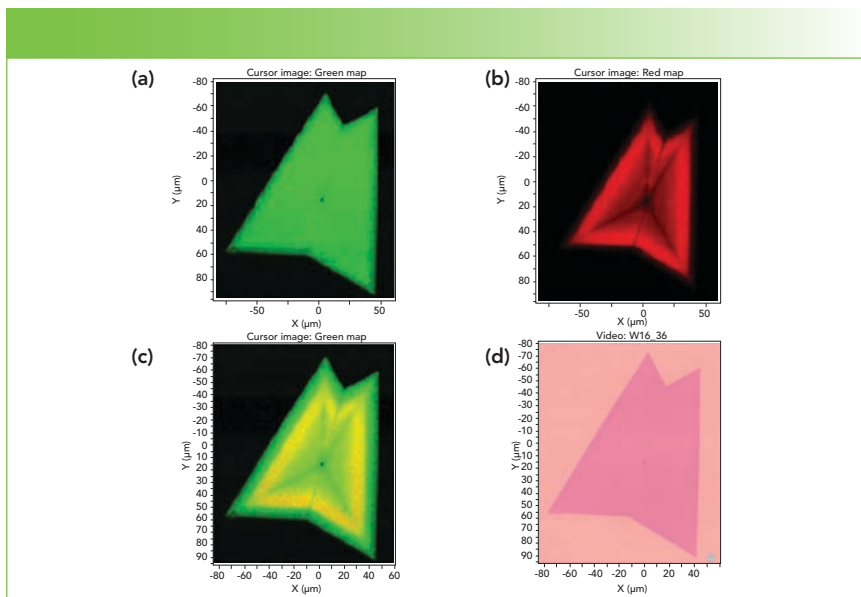


FIGURE 3: Spectral and reflected white light imaging of WS_2 : (a) Raman, (b) photoluminescence, (c) combinative Raman and photoluminescence, and (d) reflected white light image.

the most striking contrast in the PL image appears because the two-layer formation yields very weak PL emission relative to that of the single-layer portion. Also, note that the large triangle in the PL image is smaller than that of the Raman image. That is because the PL is attenuated at the perimeter of the crystal. When these two images are overlaid with normalized intensities, one obtains the combinative Raman and PL image shown in Figure 2c. The contrasting colors are the result of the spatially varying relative contributions of the Raman and PL signals. Moreover, the Raman and PL signal strengths are each normalized (minimum to maximum). That is why the perimeter of the crystal appears green from strong Raman scattering and because of the absence of or significantly attenuated PL at that location relative to the interior of the single-layer formation.

A second set of Raman, PL, combinative Raman and PL, and reflected white light images from another WS_2 crystal is shown in Figure 3. This crystal consists entirely of two single-layers of WS_2 that have grown into each other. Consequently, the Raman image in Figure 3a appears almost entirely uniform except for the dim line at the interface of the crystal growth and the small dark spot at the center that spa-

tially corresponds to the spot in the center of the reflected white light image. That small spot takes on significance in the PL image of Figure 3b that appears dark and slightly larger than that in the Raman and reflected white light images. Furthermore, dark lines of attenuated PL propagate from the center spot to each of the corners of the two crystals in a manner similar to that observed in the single crystal of Figure 2b. The contrast between the uniformity and spatial variations of the Raman and PL images, respectively is striking. When these two images are overlaid with normalized intensities, one obtains the combinative Raman and PL image shown in Figure 3c.

Here, the minimum-to-maximum color contrast generates a green-yellow combinative Raman and PL image, whereas that of Figure 2c is green-orange. The reason for this difference in color contrast is because of the normalized intensity color scaling. The Raman image of Figure 3a is of nearly uniform intensity, thereby generating a uniformly flat green Raman background for the combinative Raman and PL image. However, the Raman image of Figure 2a has spatially varying intensity because of the presence of both single and two-layer structures. Consequently, the relative Raman signal contribution under

the single-layer formation contributes less than under the three two-layer prongs in the combinative Raman and PL image of Figure 2c. The normalized PL signal in Figure 2c is relatively stronger than that of the Raman scattering of the single-layer formation resulting in the orange color in the combinative Raman and PL image. Such color contrasts demonstrate the effectiveness of combined imaging to reveal the relative Raman to PL signal strengths in different crystals.

Conclusion

Raman and PL spectroscopy reveal different aspects of the solid-state structure of 2-D materials. Combined Raman and PL imaging performed simultaneously with one instrument reveals the spatial variation of the solid-state structure and electronic properties of 2-D crystals that is not revealed in reflected white light imaging. Furthermore, examples of combinative Raman and PL images of WS_2 crystals reveal the variation of Raman to PL signal strengths within and among different crystals. The ability to image crystals through vibrational and electronic spectroscopy should allow materials scientists to better design and fabricate electronic and optoelectronic devices based upon 2-D crystals.

References

- (1) D. Jariwala, V.K. Sangwan, L.J. Lauhon, T.J. Marks and M.C. Hersam, *ACS Nano*, **8**, 1102–1120 (2014).
- (2) G. Eda and S.A. Maier, *ACS Nano*, **7**, 5660–5665 (2013).
- (3) R. Ganatra and Q. Zhang, *ACS Nano*, **8**, 4074–4099 (2014).
- (4) H. Li, J. Wu, X. Huang, G. Lu, J. Yang, X. Lu, Q. Xiong and H. Zhang, *ACS Nano*, **7**, 10344–10353 (2013).
- (5) D. Tuschel, *Spectroscopy* **30**(3), 14–29 (2015).
- (6) D. Tuschel, *Spectroscopy* **34**(9), 10–21 (2019).
- (7) D. Tuschel, *Spectroscopy* **35**(3), 9–16 (2020).



David Tuschel is a Raman Applications Scientist at Horiba Scientific, in Piscataway, New Jersey, where he works with Fran Adar. David is sharing authorship of this column with Fran. He can be reached at: SpectroscopyEdit@MMHGroup.com ●